

Optimisation and Development of a Simplified Liquid Piston Stirling Engine for Agricultural Irrigation

Mohamed Elkholy^{a,*}, Muhammad Aziz^a, Abdullah Ahmed^b, Mohamed El-Morsi^c, Omar Abdelaziz^c

^aInstitute of Industrial Science, The University of Tokyo, 4-6-1 Komaba, Meguro-ku, Tokyo 153-8505, Japan

^bDepartment of System Innovation, Osaka University, 1-1 Yamadaoka, Suita, Osaka 565-0871, Japan

^cMechanical Engineering Department, The American University in Cairo, New Cairo 11835, Egypt
 elkholy@g.ecc.u-tokyo.ac.jp

Liquid piston Stirling engine, also known as the Fluidyne engine, has been an active subject of research due to its possible integration with renewable energy technologies, like solar energy, providing a sustainable and renewable source for water pumping. Extensive research has been done on the Fluidyne engine, and previous researchers have come up with many designs to improve its efficiency. However, those developed technologies still cannot meet all the demands for practical pumping applications. This is due to the significant losses in the system, resulting in low output power (low output flow rate) and consequently low efficiency. Previous research still lacks a practical and simplified design for its utilisation in agricultural irrigation, replacing the diesel pumps that cause pollution and global warming. Thus, this paper discusses a simplified Fluidyne engine for pumping water in agriculture. The system comprises the following main components: solar Fresnel lens, hot, cold, and tuning liquid columns, regenerator, output water column, and two check valves. Comprehensive mathematical modelling for the whole system is developed, and the dynamic equations that describe each part of the system are derived and simulated using the Runge-Kutta algorithm on MATLAB. The design parameters that have significant effects on the performance of the system are optimised using the dynamic multi-objective genetic algorithm (MOFA) on MATLAB and analysed accordingly for optimum output flow rate.

1. Introduction

Many researchers have endeavored to utilise solar energy as a heating source for many applications, and one of these is external combustion engines, such as Stirling engines. Stirling engines convert thermal energy to kinetic energy through the cooling and heating of the working gas, usually air or helium, in sealed cylinders. Stirling engines mainly consist of a heating source, a working gas, a heat sink, displacer pistons, heating exchangers, and a regenerator. Their operation depends on the internal heat generated by the heat source to manipulate the pressure and temperature of the working gas and generate work (Kropiwnicki and Furmanek, 2020). The liquid piston Stirling engine, which is also referred to as the Fluidyne engine, is one type of Stirling engine that can be designed and manufactured with relatively low-cost material and tools. They are desirable for applications where free heat, low cost of manufacturing, and minimal maintenance are required. Fluidyne engines can be vital in pumping applications, especially in agriculture, where solar energy can be used as a free source of heat (Orda and Mahkamov, 2004). Fluidyne engines were invented by West in 1969. West built a prototype that was constructed from copper and brass tubes in 1971. It was reported that it achieved a maximum flow rate of 0.37 m³/h with a head of 1.6 m, heating power of 530 W, a heating temperature of 90 °C, and an efficiency of 0.35 % (West, 1987). Mosby (1978) built and tested a small-scale Fluidyne engine which revealed a pumping rate of 0.37 l/min, at a pumping head of 0.25 m, and an overall efficiency of 0.15 %. In another study, they examined the experimental results of different designs for the Fluidyne engine for pumping water, and they found out that the power output was around 20 W and an efficiency of less than 5 % (Mobsy, 1978). Mason and Stevens (2011) constructed a solar-powered Fluidyne engine powered by a Fresnel lens. Their study aimed to demonstrate the effectiveness of using a solar lens as the main source of power. The results proved that using

a solar lens is considered an effective source of power for the liquid piston Stirling engine. Yang et al. (2014) introduced the integrated two-cylinder design configuration in their research paper, and they achieved a maximum flow rate of 19 mL/min with a thermal efficiency of around 1%. Jokar and Tavakolpour (2015) proposed a novel and smart solar-powered active Stirling engine with liquid power and controllable solid displacer pistons. They also performed an optimisation scheme to find an optimum frequency and obtain maximum power for the system. Motamedi et al. (2018) proposed a design for a pressurised liquid piston Stirling engine with a solid pressure intensifier. They found that when the working gas pressure is high enough, it can push the liquid power piston to overcome the static pressure of the head, and finally, the water pumping occurs. They used the particle swarm optimisation (PSO) algorithm to study the influences of some design parameters on the hydraulic output power of the proposed system (Ahmadi et al., 2018). Fluidyne engine has been extensively studied, and previous researchers have come up with many designs to test its performance. However, previous research still lacks a practical and simplified design for the Fluidyne engine for its utilisation in agricultural irrigation, wherein it can be a perfect fit in developing countries. Moreover, the dynamic behavior of the system has not been thoroughly investigated in the previous publications, as most of the previous papers focused more on thermal and heat transfer analysis. The novelty of this study is to discuss a simplified Fluidyne engine for pumping water in agriculture that can be built with simple tools and low cost. More focus is given to studying the dynamic behavior by deriving mathematical modelling for the whole system and simulating the dynamic equations that describe each part of the system using the Runge-Kutta algorithm on MATLAB. The study also incorporates an optimisation scheme using the dynamic multi-objective genetic algorithm (MOFA) on MATLAB by producing a set of Pareto solutions for optimum output flow rate.

2. Methodology

2.1 Description of the model studied

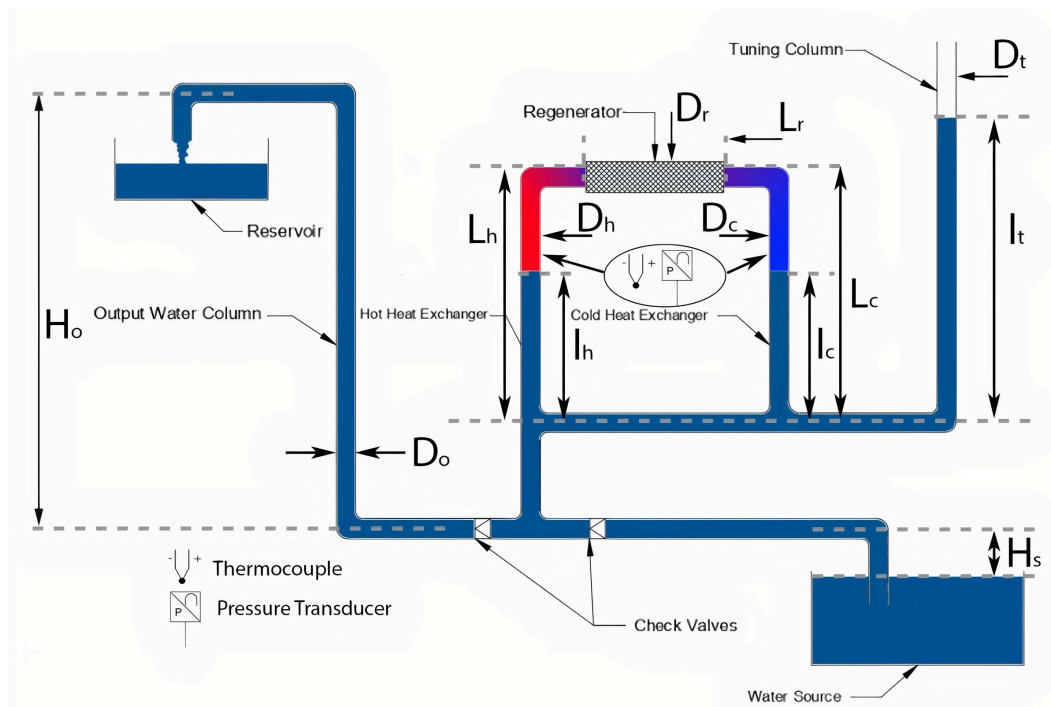


Figure 1: Schematic diagram of the model studied

The schematic model in this study, as displayed in Figure 1, includes a U-tube partially filled with water and connects to two air chambers. One of the two chambers is subjected to the heating source and is known as the hot heat exchanger, whereas the other one is exposed to the ambient air temperature and is known as the cold heat exchanger. These two heat exchangers are connected with a regenerator in the middle whose main objective is to alternately release and absorb heat during the air transfer between the hot and the cold exchangers. This helps maintain the system at an intermediate temperature between the maximum and minimum temperatures of the cycles and thus increases the thermal efficiency. The liquid column on the right is known as a tuning column. It is connected to the bottom of the U tube and opened to the atmospheric pressure,

and its main role is to balance the pressure in the system. The large column on the left is known as the output column through which the discharging occurs. Two non-returning valves are used during the suction and discharge. They open and close to allow the discharge and suction processes to occur by preventing the water movement in one direction, either to the water source or the field. Ideally, the liquid filling the U-tube mimics the solid piston's reciprocating motion (displacer piston) in the conventional Stirling Engine, which moves the working gas from the hot side to the cold side. In a more elaborated way, when the air in the hot heat exchanger gets pressurised due to the rise in the temperature, it expands, pushing the water to flow through the left valve, which is opened to the field, and discharge occurs. At the same time, the expanded air moves through the regenerator and gets cold in the cold heating exchanger, and contraction occurs, creating a vacuum that sucks the water up. The process keeps working as long as the heating source exists (which is a solar collector in our case), making the discharge and suction occur consequently.

2.2 Mathematical modelling

The mathematical modelling is divided into three main sections, the derivation for the working gas, the derivation for the hot, cold, and tuning column oscillations, and finally, the derivation for the output flow rate. For numerical simplification purposes, some assumptions are made: the working gas is considered an ideal gas, the model is developed based on the concept of dry Fluidyne, both temperatures of the cold and hot heat columns are set to be constant, and they are defined as $T_c = 20\text{ }^\circ\text{C}$ and $T_h = 120\text{ }^\circ\text{C}$, there is no heat loss between working gas and wall of the hot and cold heat exchangers, and there is no leakage and no pressure drop within the whole system. The modeling of the working gas is established based on Schmidt's theory which is used to display the variation of the gas pressure through the cycle. The control volumes for the hot, cold, and tuning columns, including the pressures applied on the top and bottom of each liquid column are used for the derivation. Considering the previous assumptions listed, the main equation that relates the variation of the working gas with the liquid oscillations that exist in the hot, cold, and tuning columns can be written as follows: (Motamedi et al., 2018).

$$\frac{dp_{wf}}{dt} = -\frac{p_{wf}}{\left(\frac{v_r}{T_r} + \frac{v_c}{T_c} + \frac{v_h}{T_h}\right)} \cdot \left(\frac{1}{T_c} \frac{dv_c}{dt} + \frac{1}{T_h} \frac{dv_h}{dt}\right) \quad (1)$$

where p_{wf} is the pressure of the working gas. v_r , v_c , v_h are the volumes of the working gas in the regenerator, the cold and hot heating exchangers. Moreover, T_r , T_c , and T_h are temperatures of the working gas in the regenerator, cold, and hot heating exchangers, correspondingly.

The equations of the hot, cold, and tuning liquid oscillations are derived using the Euler and Navier-Stokes equations, assuming inviscid incompressible flow and zero viscosity coefficient. The equations are defined as follows (Motamedi et al., 2018).

$$\rho l_h \ddot{l}_h + 8 \cdot \mu \cdot \pi \left(\frac{l_h}{A_h}\right) \cdot \dot{l}_h + \rho g l_h = (P_m - P_{wf}) \quad (2)$$

$$\rho l_c \ddot{l}_c + 8 \cdot \mu \cdot \pi \left(\frac{l_c}{A_c}\right) \cdot \dot{l}_c + \rho g l_c = (P_m - P_{wf}) \quad (3)$$

$$\rho (c_t + l_t) \ddot{l}_t + 8 \cdot \mu \cdot \pi \left(\frac{l_t + c_t}{A_t}\right) \cdot \dot{l}_t + \rho g l_t = (P_m - P_a) \quad (4)$$

where ρ is the water density, μ is the viscosity of the water, l_h , l_c , l_t are the position of the liquid in hot and cold, and tuning liquid columns, A_h , A_c , A_t are the areas of the liquid pipes of the hot and cold, and tuning liquid columns, respectively, \ddot{l}_h , \ddot{l}_c , \ddot{l}_t are the second derivative of the liquid piston positions, while c_t is the length of the horizontal pipe from the tuning column to the hot heating column, P_a is the atmospheric pressure, and P_m is the pressure applied at the bottom of the hot and cold liquid columns.

The output flow rate equation can be obtained by taking the whole system as a control volume and applying the continuity equation. Since the change in the water in the system occurs in the hot, cold, and tuning liquid columns, the change of the mass flow rate between the suction (\dot{m}_s) and discharge (\dot{m}_d) can be defined by the following equation.

$$\dot{m}_s - \dot{m}_d = \dot{l}_h * A_h * \rho + \dot{l}_c * A_c * \rho + \dot{l}_t * A_t * \rho \quad (5)$$

By defining the equation for the mass flow rate during suction $\dot{m}_s = \rho v_s A_s$ and obtaining the value of the suction velocity v_s from Bernoulli equation, the output volume flow rate during discharge (Q_0) can be represented by the Eq(6):

$$Q_0 = \left(\frac{P_{atm} - (P_m - \rho * g * L_b) A_s}{8 * \pi * \mu * L_s}\right) \cdot (\dot{l}_h * A_h + \dot{l}_c * A_c + \dot{l}_t * A_t) \quad (6)$$

3. Results and Discussion

Ode 23 Solver on MATLAB, based on the Runge-Kutta algorithm, was used to simultaneously solve the final differential equations derived for the working gas, hot, cold, and tuning columns, and the output flow rate. The results obtained were displayed in the graphs shown in Figures 2 and 3 using the design parameters listed in Table 1. It is clear that the pressure at the beginning is in an unsteady state, and that was demonstrated by the composite periodical wave, which illustrates the unsteady behavior of the system. Such behavior was expected to overcome the damping and friction forces in the Fluidyne engine's initial operation. The same behavior is also displayed in the oscillations of the hot, cold, and tuning liquid columns. The tuning liquid column is vital in the system since the tuning oscillations control the frequency of the system till reaching a steady state behavior by balancing the pressure above and below the hot and cold liquid columns. The tuning oscillations are similar in phase to the hot column oscillations and opposite to the cold column oscillations since more energy is added in the expansion stroke than what is taken in the compression stroke, meaning that the tuning momentum adds energy to the compression stroke. Also, it is noticeable that the output flow rate is discontinuous, and that was expected as the suction and discharge occur consequently according to the principle of operation of the Fluidyne Engine. The value of the output flow rate (Q_0) is calculated after integrating over the area to be $0.0347 \text{ m}^3/\text{h}$ which is equivalent to 34.7 L/h . The output power is obtained to be 14.73 W . Considering the input power for the system to be 400 W from the solar Fresnel Lens, the thermal efficiency of the system is 3.68% . The thermal efficiency of the system corresponds to the range of efficiencies commonly found in the literature which ranges from $1 - 5 \%$.

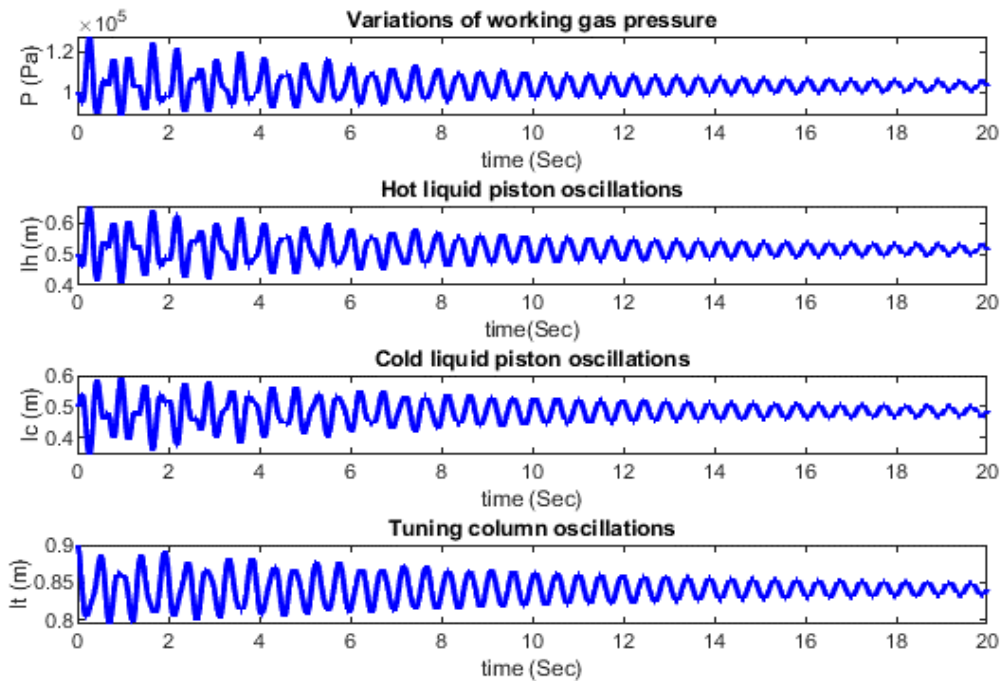


Figure 2: The oscillations behavior of the working gas pressure (P), hot, cold, and tuning liquid columns (L_h, L_c, L_t)

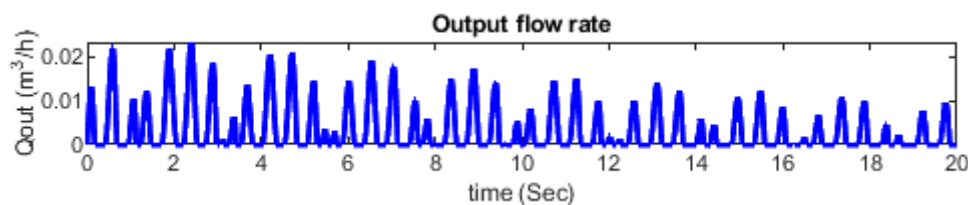


Figure 3: Oscillations behavior of the output flow rate (Q_{out})

4. Design Optimisation

Some of the design parameters that completely change the performance of the system are selected as decision variables. These decision variables are the height of the hot column (L_h), the cold column (L_c), and the length of the regenerator (L_r). Keeping in mind that the system should exhibit a stable limit cycle, three penalty functions are defined according to the amplitudes of the oscillation responses of the hot, cold, and tuning liquid.

$$F1(x) = \left| \frac{Amp_{hmax}}{Amp_{hmin}} - 1 \right| \tag{7}$$

$$F2(x) = \left| \frac{Amp_{cmax}}{Amp_{cmin}} - 1 \right| \tag{8}$$

$$F3(x) = \left| \frac{Amp_{tmax}}{Amp_{tmin}} - 1 \right| \tag{9}$$

Where Amp_{hmax} , Amp_{cmax} , Amp_{hmin} , Amp_{cmin} , Amp_{tmax} , Amp_{tmin} are the maximum and the minimum amplitudes of the hot, cold, and tuning liquid columns, respectively. It is also essential that the oscillation amplitudes of the hot and cold liquid pistons should be equal to achieve the best behavior of the system. Keeping that in mind, a fourth penalty function that should be minimised is defined as follows:

$$F4(x) = \left| \frac{mean(Amp_{hmax}, Amp_{hmin})}{mean(Amp_{hmax}, Amp_{hmin})} - 1 \right| \tag{10}$$

The fifth objective function that should be maximised is the hydraulic output power which is defined as follows:

$$F5(x) = P_0 = \rho g Q H_0 \tag{11}$$

After the five objective functions are defined, the optimal values of the three decision variables are found via an optimisation scheme using the dynamic multi-objective genetic algorithm (MOGA) on MATLAB, as displayed in Figure 4a. This optimisation algorithm was selected among all evolutionary algorithms due to its facility of use and fast convergence. For the optimisation scheme, the max population size is set to be 50 after some trial and error, the max number of generations is 300, the crossover fraction is 0.8, and the Pareto fraction is set to be 0.35. According to the results obtained from the optimisation, the objective functions were achieved after 300 generations, and the optimum values for the decision variables were found within the defined ranges. The optimum values for the decision variables obtained from the optimisation are listed in Table 2. The value of the output flow rate (Q_0) in (m³/h) is taken as a selection criterion for the optimal point from the Pareto front. In other words, the optimum Pareto point should provide the maximum output flow rate. The values of the output flow rate (Q_0) are measured at each set of points of the Pareto front, as illustrated in Figure 4b. The maximum value of the output flow rate (Q_0) is found to be 0.047 m³/h (47 L/h) at the optimum Pareto front point ($L_r = 0.7088$, $L_h = 0.6273$, $L_c = 0.7203$). The max output power is obtained to be 17.18 W. Considering the same input power for the system to be 400 W from the solar Fresnel Lens, the optimum thermal efficiency of the system is 4.29 %. The output power and thermal efficiency of the system are obtained based on the optimisation scheme are higher than previous values obtained before the optimisation.

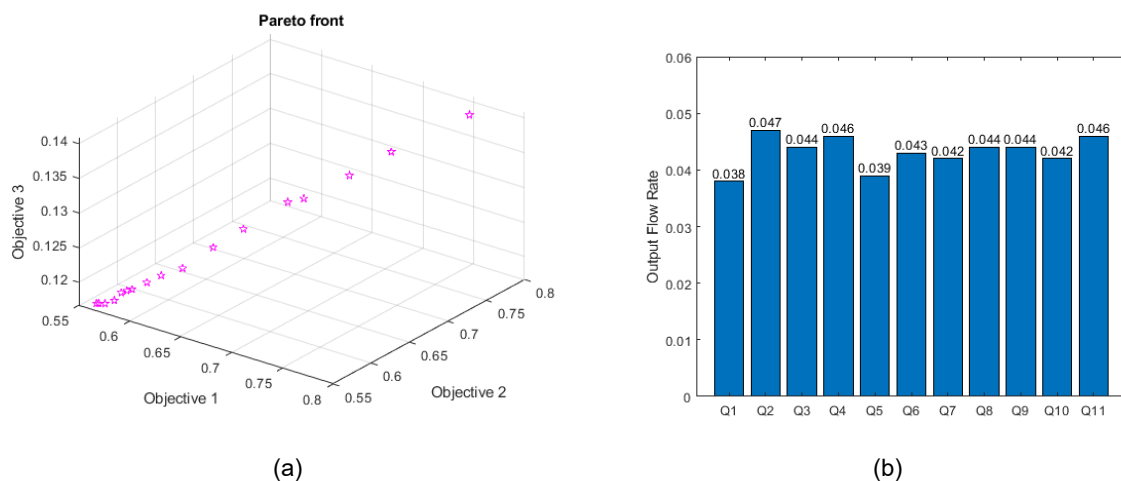


Figure 4: (a) The pareto frontier of optimal solutions from the MOGA; (b) The values of the output flow rates (Q_0) at each set for the optimum solutions listed in Table

Table 1: The paramters utilised in the model simulation on MATLAB

Parameters	Value
Dc (m)	0.025
Dh (m)	0.6273
Dt (m)	0.05
Do (m)	0.025
Ds (m)	0.025
Lr (m)	0.5
Lc (m)	0.8
Lh (m)	0.8
Lt (m)	1.5
Hs (m)	0.2
H0 (m)	1.5
Th (°c)	120
Tc (°c)	20
Tr (°c)	48
μ (Pa.s)	10^{-4}
Patm (Pa)	10^5
g (m/s ²)	9.81
ρ (kg/m ³)	1000

Table 2: Optimal solutions obtained from the optimisation for L_r , L_h , and L_c

L_r (m)	L_h (m)	L_c (m)
0.774	0.6965	0.7383
0.7088	0.6273	0.7203
0.7139	0.6684	0.7273
0.7163	0.6392	0.7067
0.7607	0.6795	0.7554
0.7505	0.6651	0.7470
0.7514	0.6818	0.7514
0.7343	0.6465	0.7505
0.7369	0.7110	0.7492
0.7497	0.6579	0.7518
0.7263	0.6395	0.7227

5. Conclusion

This study presented modeling and simulation of a simple liquid piston Stirling engine for Agricultural Irrigation. Considering the simplicity of the model studied, the results are still promising that could inspire future work and raise greater awareness of utilising Fluidyne Engine as a sustainable and renewable source for water pumping for agriculture irrigation in developing countries. Future work may consider performing sensitivity analysis of integrating solar energy with the Fluidyne engine and study how the variation of the solar annual radiation affects the performance of such engines and the amount of the output flow rate that can be obtained when these engines are utilised for pumping water in the agriculture field. Also, a feasibility analysis could be performed to compare such a concept with existing pumping technologies in terms of the energy saved, the overall cost, and the reduction of emission of greenhouse gases.

References

- Ahmadi R., Jokar H., Motamedi M., 2018, A solar pressurizable liquid piston stirling engine: Part 2, optimisation and development, *Energy*, 164, 1200.
- Genetic Algorithm:multi-objective genetic algorithm (MOGA), 2021, The Math Works, Inc., MATLAB, version 2021b < <https://www.mathworks.com/> > accessed 11.12.2021.
- Jokar H., Tavakolpour A., 2015. A novel solar-powered active low temperature differential Stirling pump, *Renewable Energy*, 81,319-337.
- Kropiwnicki J., Furmanek M., 2020, A Theoretical and Experimental Study of Moderate Temperature Alfa Type Stirling Engines, *Energies*,13 (7),16.
- Mason J., Stevens, J., 2011, Characterization of a solar-powered fluidyne test bed. *Sustainable Energy Technologies and Assessments*, 8,1-8.
- Mosby D. C., The fluidyne heat engine, Master's thesis, Naval Postgraduate School, United States. < <https://www.osti.gov/biblio/6190276-fluidyne-heat-engine-master-thesis> > accessed 22.03.2021.
- Motamedi M., Ahmadi R., Jokar H., 2018, A solar pressurizable liquid piston stirling engine: Part 1, mathematical modeling, simulation and validation. *Energy*, 155, 796-814.
- Orda E., Mahkamov K., 2004, Development of Low-tech Solar Thermal Water Pumps for Use in Developing Countries, *Journal of Solar Energy Engineering*,126 (2), 768–773.
- Runge Kutta Algorithm:ode23 solver on MATLAB, 2021, The Math Works, Inc., MATLAB, version 2021b <<https://www.mathworks.com/>> accessed 10.08.2021.
- West C. D., 1987, Stirling engines and irrigation pumping < <https://www.osti.gov/biblio/6281973-stirling-engines-irrigation-pumping> > accessed 21.03.2021.
- Yang N., Rickard R., Pluckter, K., Sulchek T., 2014, Integrated two-cylinder liquid piston Stirling engine, *Applied Physics Letters*, 105 (14),143903.